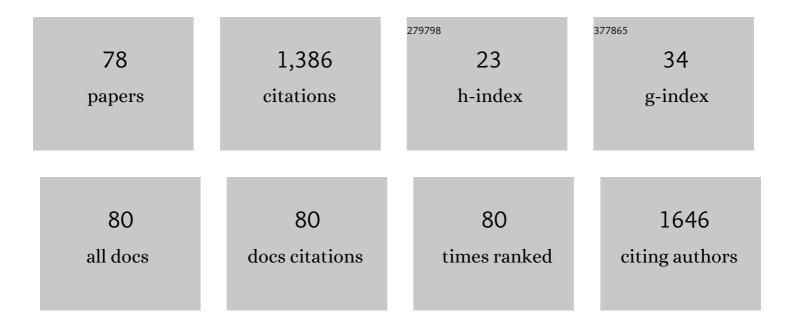
Anne Sophie Bouvier

List of Publications by Year in descending order

Source: https://exaly.com/author-pdf/4886353/publications.pdf Version: 2024-02-01



#	Article	IF	CITATIONS
1	Warm storage for arc magmas. Proceedings of the National Academy of Sciences of the United States of America, 2016, 113, 13959-13964.	7.1	88
2	Slab-Derived Fluids in the Magma Sources of St. Vincent (Lesser Antilles Arc): Volatile and Light Element Imprints. Journal of Petrology, 2008, 49, 1427-1448.	2.8	87
3	Li isotopes and trace elements as a petrogenetic tracer in zircon: insights from Archean TTGs and sanukitoids. Contributions To Mineralogy and Petrology, 2012, 163, 745-768.	3.1	78
4	Time and duration of chondrule formation: Constraints from 26Al-26Mg ages of individual chondrules. Geochimica Et Cosmochimica Acta, 2019, 244, 416-436.	3.9	74
5	Reconstruction of multiple P-T-t stages from retrogressed mafic rocks: Subduction versus collision in the Southern BrasĀlia orogen (SE Brazil). Lithos, 2017, 294-295, 283-303.	1.4	56
6	Contrasting hydrological processes of meteoric water incursion during magmatic–hydrothermal ore deposition: An oxygen isotope study by ion microprobe. Earth and Planetary Science Letters, 2016, 451, 263-271.	4.4	55
7	Experimental determination of melt interconnectivity and electrical conductivity in the upper mantle. Earth and Planetary Science Letters, 2017, 463, 286-297.	4.4	44
8	Dynamic growth of garnet in granitic magmas. Geology, 2012, 40, 171-174.	4.4	40
9	Zircon petrochronology reveals the timescale and mechanism of anatectic magma formation. Earth and Planetary Science Letters, 2018, 495, 213-223.	4.4	40
10	Silicate melt inclusions in the new millennium: A review of recommended practices for preparation, analysis, and data presentation. Chemical Geology, 2021, 570, 120145.	3.3	40
11	Heterogeneous melt and hypersaline liquid inclusions in shallow porphyry type mineralization as markers of the magmatic-hydrothermal transition (Cerro de Pasco district, Peru). Chemical Geology, 2016, 447, 93-116.	3.3	38
12	Evidence for cavity-dwelling microbial life in 3.22 Ga tidal deposits. Geology, 2016, 44, 51-54.	4.4	38
13	Light elements, volatiles, and stable isotopes in basaltic melt inclusions from Grenada, Lesser Antilles: Inferences for magma genesis. Geochemistry, Geophysics, Geosystems, 2010, 11, .	2.5	33
14	The dark side of zircon: textural, age, oxygen isotopic and trace element evidence of fluid saturation in the subvolcanic reservoir of the Island Park-Mount Jackson Rhyolite, Yellowstone (USA). Contributions To Mineralogy and Petrology, 2018, 173, 1.	3.1	31
15	Quartz Reference Materials for Oxygen Isotope Analysis by <scp>SIMS</scp> . Geostandards and Geoanalytical Research, 2017, 41, 69-75.	3.1	30
16	Fluid Inputs to Magma Sources of St. Vincent and Grenada (Lesser Antilles): New Insights from Trace Elements in Olivine-hosted Melt Inclusions. Journal of Petrology, 2010, 51, 1597-1615.	2.8	29
17	First Lu-Hf, δ18O and trace elements in zircon signatures from the Statherian Espinhaço anorogenic province (Eastern Brazil): geotectonic implications of a silicic large igneous province. Brazilian Journal of Geology, 2018, 48, 735-759.	0.7	29
18	Mineralized breccia clasts: a window into hidden porphyry-type mineralization underlying the epithermal polymetallic deposit of Cerro de Pasco (Peru). Mineralium Deposita, 2018, 53, 919-946.	4.1	26

Anne Sophie Bouvier

#	Article	IF	CITATIONS
19	Multispecies Diffusion of Yttrium, Rare Earth Elements and Hafnium in Garnet. Journal of Petrology, 2020, 61, .	2.8	26
20	SIMS chlorine isotope analyses in melt inclusions from arc settings. Chemical Geology, 2017, 449, 112-122.	3.3	25
21	Weekly to monthly time scale of melt inclusion entrapment prior to eruption recorded by phosphorus distribution in olivine from mid-ocean ridges. Geology, 2017, 45, 1059-1062.	4.4	25
22	Zircon petrochronology in large igneous provinces reveals upper crustal contamination processes: new U–Pb ages, Hf and O isotopes, and trace elements from the Central Atlantic magmatic province (CAMP). Contributions To Mineralogy and Petrology, 2021, 176, 1.	3.1	25
23	Short magmatic residence times of quartz phenocrysts in Patagonian rhyolites associated with Gondwana breakup. Geology, 2016, 44, 67-70.	4.4	23
24	Fluid mixing as primary trigger for cassiterite deposition: Evidence from in situ δ18O-δ11B analysis of tourmaline from the world-class San Rafael tin (-copper) deposit, Peru. Earth and Planetary Science Letters, 2021, 563, 116889.	4.4	23
25	The Gondwanan margin in West Antarctica: Insights from Late Triassic magmatism of the Antarctic Peninsula. Gondwana Research, 2020, 81, 1-20.	6.0	22
26	A modern scleractinian coral with a two-component calcite–aragonite skeleton. Proceedings of the National Academy of Sciences of the United States of America, 2021, 118, .	7.1	22
27	Biotite Reference Materials for Secondary Ion Mass Spectrometry ¹⁸ 0/ ¹⁶ 0 Measurements. Geostandards and Geoanalytical Research, 2017, 41, 243-253.	3.1	17
28	Carbon partitioning between metal and silicate melts during Earth accretion. Earth and Planetary Science Letters, 2021, 554, 116659.	4.4	17
29	Oxygen isotope speedometry in granulite facies garnet recording fluid/melt–rock interaction (SÃ,r) Tj ETQq1 I	1 0.78431 3.4	4 rgBT /Over
30	The role of crustal melting in the formation of rhyolites: Constraints from SIMS oxygen isotope data (Chon Aike Province, Patagonia, Argentina). American Mineralogist, 2018, 103, 2011-2027.	1.9	15
31	Diffusion anisotropy of Ti in zircon and implications for Ti-in-zircon thermometry. Earth and Planetary Science Letters, 2022, 578, 117317.	4.4	15
32	Pervasive Eclogitization Due to Brittle Deformation and Rehydration of Subducted Basement: Effects on Continental Recycling?. Geochemistry, Geophysics, Geosystems, 2018, 19, 865-881.	2.5	14
33	Low Temperature Serpentinite Replacement by Carbonates during Seawater Influx in the Newfoundland Margin. Minerals (Basel, Switzerland), 2020, 10, 184.	2.0	14
34	New Reference Materials and Assessment of Matrix Effects for SIMS Measurements of Oxygen Isotopes in Garnet. Geostandards and Geoanalytical Research, 2020, 44, 459-471.	3.1	14
35	Evaluation of potential monazite reference materials for oxygen isotope analyses by SIMS and laser assisted fluorination. Chemical Geology, 2017, 450, 199-209.	3.3	13

36 Multi fluid-flow record during episodic mode I opening: A microstructural and SIMS study (Cotiella) Tj ETQq0 0 0 rgBT /Overlock 10 Tf 50

#	Article	IF	CITATIONS
37	Origin of Monte Rosa whiteschist from in-situ tourmaline and quartz oxygen isotope analysis by SIMS using new tourmaline reference materials. American Mineralogist, 2019, 104, 1503-1520.	1.9	13
38	Tracing of Cl input into the sub-arc mantle through the combined analysis of B, O and Cl isotopes in melt inclusions. Earth and Planetary Science Letters, 2019, 507, 30-39.	4.4	13
39	A Method for Secondary Ion Mass Spectrometry Measurement of Lithium Isotopes in Garnet: The Utility of Glass Reference Materials. Geostandards and Geoanalytical Research, 2021, 45, 477-499.	3.1	13
40	A NanoSIMS Investigation on Timescales Recorded in Volcanic Quartz From the Silicic Chon Aike Province (Patagonia). Frontiers in Earth Science, 2018, 6, .	1.8	12
41	Diffusion of calcium in forsterite and ultra-high resolution of experimental diffusion profiles in minerals using local electrode atom probe tomography. Geochimica Et Cosmochimica Acta, 2019, 265, 85-95.	3.9	11
42	Reactive fluid infiltration along fractures: Textural observations coupled to in-situ isotopic analyses. Earth and Planetary Science Letters, 2019, 519, 264-273.	4.4	11
43	Episodic fluid flow in an eclogite-facies shear zone: Insights from Li isotope zoning in garnet. Geology, 2022, 50, 746-750.	4.4	10
44	Assessing the impact of diagenesis on foraminiferal geochemistry from a low latitude, shallow-water drift deposit. Earth and Planetary Science Letters, 2020, 545, 116390.	4.4	9
45	Tracing sulfur sources in the crust via SIMS measurements of sulfur isotopes in apatite. Chemical Geology, 2021, 579, 120242.	3.3	9
46	Degassing from magma reservoir to eruption in silicic systems: The Li elemental and isotopic record from rhyolitic melt inclusions and host quartz in a Yellowstone rhyolite. Geochimica Et Cosmochimica Acta, 2022, 326, 56-76.	3.9	9
47	Melt Extraction Zones in Shallow Arc Plutons: Insights from Fisher Lake Orbicules (Sierra Nevada,) Tj ETQq1 1 0.	.784314 rg 2.8	gBT <mark>/</mark> Overlock
48	Development and Reâ€Evaluation of Tourmaline Reference Materials for In Situ Measurement of Boron δ Values by Secondary Ion Mass Spectrometry. Geostandards and Geoanalytical Research, 2020, 44, 593-615.	3.1	8
49	Highâ€spatialâ€resolution measurements of iron isotopes in pyrites by secondary ion mass spectrometry using the new Hyperionâ€II radioâ€frequency plasma source. Rapid Communications in Mass Spectrometry, 2021, 35, e8986.	1.5	8
50	Tracking fluid mixing in epithermal deposits – Insights from in-situ δ180 and trace element composition of hydrothermal quartz from the giant Cerro de Pasco polymetallic deposit, Peru. Chemical Geology, 2021, 576, 120277.	3.3	8
51	Significance of OH, F and Cl content in biotite during metamorphism of the Western Adamello contact aureole. Contributions To Mineralogy and Petrology, 2018, 173, 1.	3.1	7
52	Experimental Melting of Hydrothermally Altered Rocks: Constraints for the Generation of Low-δ18O Rhyolites in the Central Snake River Plain. Journal of Petrology, 2019, 60, 1881-1902.	2.8	7
53	Li isotope zoning in garnet from Franciscan eclogite and amphibolite: The role of subduction-related fluids. Geochimica Et Cosmochimica Acta, 2020, 286, 198-213.	3.9	7
54	The fate of a travertine record: Impact of early diagenesis on the Yâ€10 core (Mammoth Hot Springs,) Tj ETQq0	0 0 rgBT /	Overlock 10 T

#	Article	IF	CITATIONS
55	Carbonatitic dykes during Pangaea transtension (Pelagonian Zone, Greece). Lithos, 2018, 302-303, 329-340.	1.4	4
56	Accurate Measurements of H ₂ O, F and Cl Contents in Biotite Using Secondary Ion Mass Spectrometry. Geostandards and Geoanalytical Research, 2018, 42, 523-537.	3.1	4
57	Grain scale processes recorded by oxygen isotopes in olivine-hosted melt inclusions from two MORB samples. Chemical Geology, 2019, 511, 11-20.	3.3	4
58	SIMS analysis of Si isotope for radiolarian test in Mesozoic bedded chert, Inuyama, central Japan. Bulletin of the Geological Survey of Japan, 2020, 71, 331-353.	0.7	3
59	Chlorine isotope behavior in subduction zone settings revealed by olivine-hosted melt inclusions from the Central America Volcanic Arc. Earth and Planetary Science Letters, 2022, 581, 117414.	4.4	2
60	Interplay between fluid circulation and Alpine metamorphism in the Monte Rosa whiteschist from white mica and quartz in situ oxygen isotope analysis by SIMS. American Mineralogist, 2022, 107, 860-872.	1.9	1
61	An Integrated O ₂ -Hf-U/Pb Isotope Study of Zircon on Crustal Growth in the Yavapai Province of Colorado. , 2020, , .		1
62	Oxygen isotope analysis of Mesozoic radiolarites using SIMS. Bulletin of the Geological Survey of Japan, 2020, 71, 355-393.	0.7	1
63	Deciphering Degassing and Source Effects in Cl Isotopes in Melt Inclusions: The Possible Role of Amphibole in the Magma Source of Stromboli (Aeolian Island Arc). Frontiers in Earth Science, 2022, 9, .	1.8	1
64	Melt inclusion formation during olivine recrystallization: Evidence from stable isotopes. Earth and Planetary Science Letters, 2022, 592, 117638.	4.4	1
65	REACTIVE FLUID-FLOW AND STABLE ISOTOPE EXCHANGE RELATED TO HYDROTHERMAL VEINS IN CARBONATE XENOLITHS: A COUPLED CL IMAGING AND SIMS STUDY. , 2016, , .		0
66	OXYGEN ISOTOPE CONSTRAINTS ON CRUSTAL MELTING: SIMS DATA FROM JURASSIC RHYOLITES OF THE CHON AIKE PROVINCE (PATAGONIA, ARGENTINA). , 2016, , .		0
67	MULTI FLUID-FLOW EVENTS DURING MODE I OPENING: A MICROSTRUCTURAL AND SIMS STUDY. , 2016, , .		0
68	WATER CONTENT OF BIOTITE AS MONITOR OF CHANGE IN WATER ACTIVITY. , 2016, , .		0
69	IN-SITU OXYGEN ISOTOPE STUDY OF TOURMALINE AND QUARTZ: INSIGHTS INTO THE PROGRADE TEMPERATURE HISTORY. , 2017, , .		0
70	STOPPING CRYSTAL CLOCKS: THE ROLE OF ELECTRONS IN ARRESTING DIFFUSION OF LITHIUM IN SUBDUCTION ZONE GARNETS. , 2019, , .		0
71	In situ High Resolution Measurements of Fe Isotope Composition in Micro-Pyrite Using Hyperion Radio Frequency Source on IMS 1280 HR2. , 2020, , .		0
72	Improving our understanding of LIP emplacement ages using petrology, thermal modelling, and geochemistry of zircon crystals: a case study from the Central Atlantic Magmatic Province. , 2021, , .		0

#	Article	IF	CITATIONS
73	Tracking Volatile Degassing of an Explosive, Rhyolitic Eruption Using Lithium Isotopes. , 2020, , .		Ο
74	A positive iron isotope excursion recorded in micropyrites at the Smithian-Spathian (Early Triassic) boundary. , 2021, , .		0
75	Modern and Ancient Hydrosphere-Rock Interactions Constrained from Triple Oxygen Isotope and <i>in situ</i> δ ¹ ⁸ 0 Measurements. , 2020, , .		0
76	SIMS Analysis of Si Isotope for Radiolarian Test in Mesozoic Bedded Chert, Inuyama, Central Japan. , 2020, , .		0
77	Link between Fluids and Stable Isotope Disequilibrium between Melt Inclusions and Host Olivine. , 2020, , .		0
78	Differential record of pre- and syn-eruptive degassing of a large rhyolitic system recorded by Li, H, and Î7Li diffusion between quartz, melt inclusions and groundmass glasses. , 2021, , .		0